JOURNAL OF PLASTIC SURGERY AND HAND SURGERY
2020, VOL. 54, NO. 3, 137–144
https://doi.org/10.1080/2000656X.2019.1710710

ARTICLE

The effect of the macrophage migration inhibitory factor (MIF) on excisional wound healing *in vivo*

Bong-Sung Kim[a,b], Benjamin Breuer[a], Kevin Arnke[b], Tim Ruhl[a], Tanja Hofer[a], David Simons[a,c], Matthias Knobe[d,e], Bergita Ganse[d], Marco Guidi[b], Justus P. Beier[a], Paul C. Fuchs[f], Norbert Pallua[a,g], Jürgen Bernhagen[h,i] and Gerrit Grieb[a,j]

[a]Department of Plastic and Reconstructive Surgery, Hand Surgery – Burn Center, RWTH Aachen University Hospital, Aachen, Germany; [b]Department of Plastic Surgery and Hand Surgery, University Hospital Zurich, Zurich, Switzerland; [c]German Cancer Research Center (DKFZ), Heidelberg, Germany; [d]Department of Orthopaedic Trauma, RWTH Aachen University Hospital, Aachen, Germany; [e]Division of Trauma Surgery, Kantonsspital Luzern, Luzern, Switzerland; [f]Department of Plastic Surgery, Hand Surgery – Burn Center, Cologne-Merheim Medical Center, Witten/Herdecke University, Cologne, Germany; [g]Aesthetic Elite International – Private Clinic, Düsseldorf, Germany; [h]Chair of Vascular Biology, Institute for Stroke and Dementia Research (ISD), LMU University Hospital, Ludwig-Maximilians-University (LMU) Munich, Germany; [i]Munich Cluster for Systems Neurology (SyNergy), Munich, Germany; [j]Department of Plastic Surgery and Hand Surgery, Gemeinschaftskrankenhaus Havelhoehe, Teaching Hospital of the Charité University, Berlin, Germany

ABSTRACT

Background: The macrophage migration inhibitory factor (MIF) has been determined as a cytokine exerting a multitude of effects in inflammation and angiogenesis. Earlier studies have indicated that MIF may also be involved in wound healing and flap surgery. *Methods:* We investigated the effect of MIF in an excisional wound model in wildtype, *Mif*$^{-/-}$ and recombinant MIF treated mice. Wound closure rates as well as the macrophage marker Mac-3, the pro-inflammatory cytokine tumor necrosis factor α (TNFα) and the pro-angiogenic factor von Willebrand factor (vWF) were measured. Finally, we used a flap model in *Mif*$^{-/-}$ and WT mice with an established perfusion gradient to identify MIF's contribution in flap perfusion. *Results:* In the excision wound model, we found reduced wound healing after MIF injection, whereas *Mif* deletion improved wound healing. Furthermore, a reduced expression of Mac-3, TNFα and vWF in *Mif*$^{-/-}$ mice was seen when compared to WT mice. In the flap model, *Mif*$^{-/-}$ knockout mice showed mitigated flap perfusion with lower hemoglobin content and oxygen saturation as measured by O_2C measurements when compared to WT mice. *Conclusions:* Our data suggest an inhibiting effect of MIF in wound healing with increased inflammation and perfusion. In flaps, by contrast, MIF may contribute to flap vascularization.

Abbreviations: COX2: cyclooxygenase 2; EPC: endothelial progenitor cell; IFN-γ: interferon-γ; IL: interleukin; MIF: macrophage migration inhibitory factor; Mif$^{-/-}$: MIF knockout; O_2C: oxygen to see; rHb: relative hemoglobin content; SaO_2: oxygen saturation; TNFα: tumor necrosis factor α; vWF: von Willebrand facto

ARTICLE HISTORY
Received 21 August 2019
Revised 8 December 2019
Accepted 21 December 2019

KEYWORDS
MIF; wound healing; flap model; excisional wound; perfusion; hypoxia; macrophages

Introduction

Wound healing is a complex body response for tissue restoration after injury. While physiological wound repair processes result in scar formation after a short time period, non-healing wounds present a serious threat to patients and global healthcare systems. Non-healing wounds are often caused by impaired wound perfusion due to etiologies such as diabetic angiopathy or peripheral arterial disease resulting in tissue hypoxia [1]. Furthermore, a prolonged tissue inflammation due to many intrinsic and extrinsic factors such as metabolic diseases, tension to the wound, bacterial infection further inhibits wound healing.

In the context of wound healing, the macrophage migration inhibitory factor (MIF), a cytokine that was first described in delayed-type hypersensitivity [2], may be a relevant factor.

On a molecular level, MIF interacts with the chemokine receptors CXCR2 and CXCR4 [3], CXCR7 [4] and the receptor complex CD74/CD44 [5–7]. As a central albeit ambiguous mediator of inflammation, MIF has a deleterious impact on a variety of diseases including malignancies, inflammatory, autoimmune as well as metabolic diseases [8]. MIF orchestrates tissue inflammation and tissue perfusion *via* different pathways.

First, MIF is an up-stream regulator and a strong inducer of pro-inflammatory cascades and has been reported earlier to induce the release of key inflammatory mediators such as tumor necrosis factor (TNF)α, interleukin (IL)-1β, IL-6, nitric oxide, cyclooxygenase (COX)2, and interferon (IFN)-γ [9,10]. Second, MIF acts as a chemokine with the ability to facilitate monocyte and T-cell recruitment and to promote the migration of endothelial progenitor cells (EPCs) [3,11,12]. We previously observed increased MIF-dependent infiltration of monocytes and macrophages in adipose tissue adjacent to inflammatory non-healing wounds [13]. Third, MIF is involved in angiogenesis which is particularly well described in the context of tumor progression [7].

The MIF protein is detected ubiquitously in all skin layers [14] and expressed during all stages of wound healing [15]. Due to MIF's multi-faceted function with pro-inflammatory properties and

CONTACT Bong-Sung Kim bong-sung.kim@usz.ch, bong.kim@rwth-aachen.de Department of Plastic Surgery and Hand Surgery, University Hospital Zurich, Raemistrasse 100, 8091 Zurich, Switzerland

its role in tissue perfusion, it may exert different effects in wound repair.

In the present study, we investigated MIF's effect on wound repair in more detail. To differentiate wound healing under normal, healthy conditions with regular perfusion and pathological conditions with restricted blood perfusion as found in many patients experiencing wound healing disorders, we performed two separate experiments. We first investigated the healing course in an excisional wound model (Experiment 1) under regular perfusion of the wounds. In the second model, a cutaneous flap was raised on the back of the mice (Experiment 2) to create a perfusion gradient in the flap and simulate restricted blood perfusion.

Methods

Animals

Eight to 12-week-old female C57BL/6 WT ($n = 24$) and *Mif*$^{-/-}$ ($n = 12$) mice were used in the present study. All WT mice were purchased from Charles River Laboratories (Sulzfeld, Germany). The precise generation of *Mif*$^{-/-}$ mice was reported previously [15]. Animals were held in the facilities of the Institute of Laboratory Animal Science and Central Animal Testing Laboratory of the RWTH Aachen University Hospital. All experiments were approved by the local governmental authorities (State Office for Nature, Environment and Consumer Protection North Rhine-Westphalia, LANUV, protocol number 9.93.2.10.35.07.285). Mice were housed under a 12:12 h light dark cycle, in standard cages under pathogen-free conditions with access to water and food *ad libitum*. Twenty-four mice were used in the wound model and 12 mice were used in the flap model, respectively.

Anesthesia and surgical preparation

All surgeries were performed under sterile conditions. Mice were anesthetized *via* a sedation with 2% Isoflurane by drop jar method followed by 100 mg/kg bodyweight ketamine and 10 mg/kg bodyweight xylazine diluted in 100 µl PBS. The back of the animals was shaved, prepped and draped by sterile sheets. For maintenance of body temperature, the animal was laid on a heat pad during surgery. Extremities were fixed by sterile tapes.

Excisional wound model

To examine MIF's role in wound healing we performed an excisional wound model. Excisional wounds were created on the dorsum (proximal row: 2 cm caudal of the ears; distal row: 5 cm caudal of the proximal row; Figure 1(a)) by a 6 mm punch biopsy device (Stiefel, Munich, Germany). The skin was excised down to the fascia and wounds were allowed to heal by secondary intention under sterile gauze dressings. Sterile gauzes were applied to the wound immediately after the surgery and were fixed by a transparent dressing (Tegaderm, 3 M, Neuss, Germany) for 24 h. Two groups of mice received additional injection of 500 ng/100 µl of recombinant MIF dissolved in saline [16] or the equal volume of saline into the wound edges, at the end of the operation as well as on days 1 and 2 after surgery. Operated animals were housed individually. On days 1, 3, 7 and 14, the diameter of wounds of each individual was carefully measured by taking three pictures which were then evaluated by the software GIMP (GIMP Development Team, CA, USA). A tape measure was included in each photograph to calibrate linear dimensions [17]. The initial wound diameter (6 mm) was taken as 100%, wound healing progress was calculated as a percentage of those on day 0. On days 3, 7 and 14, two mice of each group were euthanized by a lethal dose of isoflurane (inhalation), followed by complete wound excision for histological examination.

Immunofluorescence

Tissue samples were fixed in 4% paraformaldehyde for 24 h. After dehydration with ethanol, the tissue was embedded in paraffin. Tissue blocks were then cut on a microtome (Histoslide, Reichert Jung, Munich, Germany) and standard Hematoxylin/eosin (HE) staining was performed. Cells that infiltrated the wounds were photographed with the software Diskus (Hilgers Technisches Büro, Königswinter, Germany). At 200-fold magnification, random squares measuring $400 \times 400\,nm^2$ were analyzed by blinded observers. Numbers of counted cells were averaged and extrapolated to an area of $1\,mm^2$.

Mac-3 (BD Pharmingen, Heidelberg, Germany) – (Lysosomal-associated membrane protein 2) an intracellular marker for murine

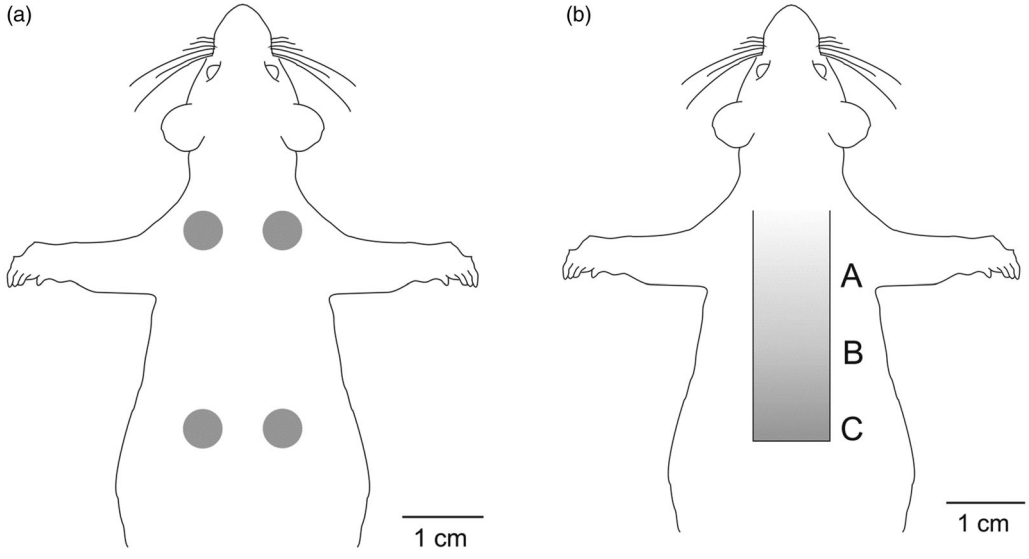

Figure 1. Experimental setup: Dorsal view on location and dimension of (a) excisional wounds. Tissue was wounded with a punch biopsy device, diameter = 0.6 mm. In another experiment (b), random pattern flaps with the size of $1 \times 3\,cm^2$ (Experiment 2, restricted perfusion) were divided into three zones of equal extends differing in oxygen supply, indicated by grey intensity: Proximal zone A (white – light grey) with regular in contrast to distal zone C with gradually decreasing perfusion (dark grey).

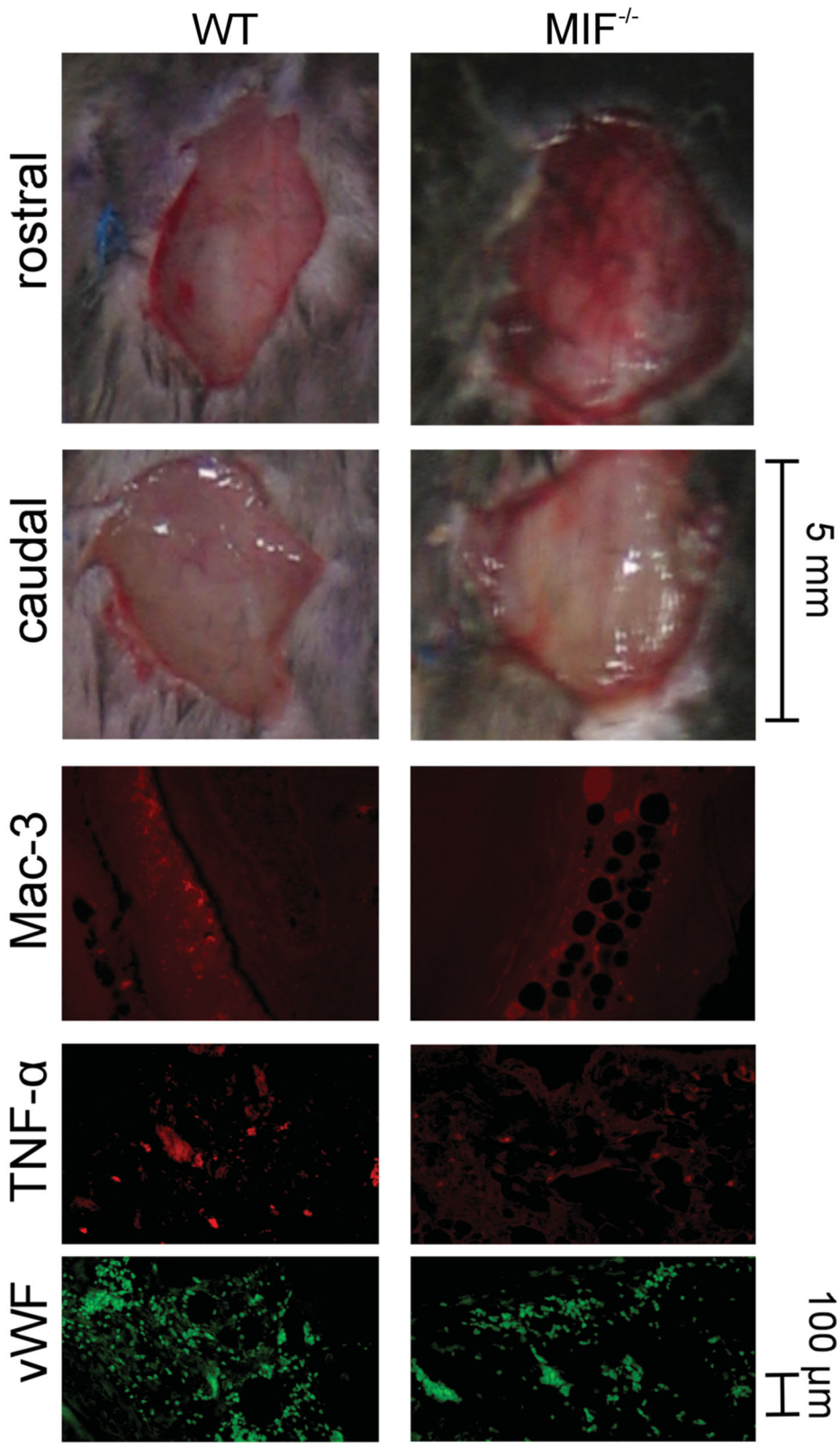

Figure 2. Experimental procedure of excisional wound model. First row: representative photos of excisional wounds from WT (left column) and *Mif*$^{-/-}$ mice (right column) on day 1 after the surgery. Dissected wounds were analyzed for second row: Mac-3, third row: TNFα and fourth row: vWF. Scale bar: 5 mm for wound images, scale bar: 100 µm for microscopic photos of immune-labelled cells.

macrophage differentiation – with an Alexa 546 secondary antibody (Invitrogen™, Frankfurt a. M., Germany), the pro-inflammatory cytokine tumor necrosis factor α (TNFα, R&D Systems GmbH, Wiesbaden, Germany) with an Alexa 555 secondary antibody (Invitrogen™, Frankfurt a. M., Germany), and von Willebrand factor (vWF), a glycoprotein involved in hemostasis and

vascularization (Genetex Inc., Irvine, CA, USA) with an Alexa 488 secondary antibody (Invitrogen™, Frankfurt a. M., Germany) was stained (Figure 2). Images were taken under a microscope. The fluorescent area was calculated as percentage of total area by the image processing software GIMP, Version 2.6.11. The evaluation of the stainings was done in a blinded way.

Flap model

To additionally investigate MIF-dependent wound repair under restricted perfusion, we examined wounds in a flap model that established a perfusion gradient. We compared the wound healing characteristics in WT mice ($n = 6$) and in *MIF*$^{-/-}$ mice ($n = 6$).

A random pattern flap measuring 1×3 cm was elevated on the dorsum of the mice (Figure 1(b)) after careful establishment of flap dimensions in preliminary studies. The flap model was chosen in a way, that due to an ischemic gradient from A to C the distal parts of zone C became necrotic between day 3 and 7 in WT mice. The necrosis provided evidence for a clinically relevant ischemia in the distal parts of the flap. After incision of the skin, the flap was prepared down to the muscle fascia and the flap was incised on the lateral and distal borders. The flap was then raised from the caudal to rostral direction on the muscle fascia with blood circulation granted by a perfusion from the proximal base of the flap. The flap was divided into three equal zones with zone A being the proximal third, zone B being the central third, and zone C representing the distal third of the flap (Figure 1(b)). By disconnecting the flap on the lateral and distal border, a perfusion gradient was established with its highest flow in the proximal third and lowest flow on the distal third. After full mobilization of the flap, it was re-attached to its original donor site and fixed by a braided 5.0 suture. The flap was covered by sterile gauze for the first 24 h after surgery. Flaps of 2 mice were completely excised for histological evaluation at days 3, 7 and 14, respectively.

The morphology of the flap was monitored macroscopically and evaluated in a blinded way. The O_2C device (oxygen to see, LEA Medizintechnik GmbH, Gießen, Germany) is a combination of a tissue spectrometer and a laser Doppler flowmeter. The O_2C device was used as a to evaluate the flap perfusion by a non-invasive method and thereby reduce the suffering of the animals. The blood flow, relative hemoglobin content (rHb), and oxygen saturation (SaO_2) of the flap was monitored daily by the O_2C device. The parameters were measured blinded in a tissue depth of approximately 2 mm by a probe (model: CF-2).

Statistical analysis

Data of experiments were averaged and presented as bars ± SEM. If appropriate, statistical differences were evaluated between the different types of treatment (saline and MIF injection) and the genetic background (WT and *Mif*$^{-/-}$). Data were analyzed for normality using the Kolmogorov-Smirnov test. Non-normally distributed data were presented as box-plots ± 25/75% box boundaries. Pairwise comparison was performed using the Kruskal-Wallis H-test followed by Mann-Whitney U-tests after Bonferroni correction (SPSS 22, SPSS Inc., Chicago, IL, USA). Statistical significance was accepted if $^*p < 0.05$.

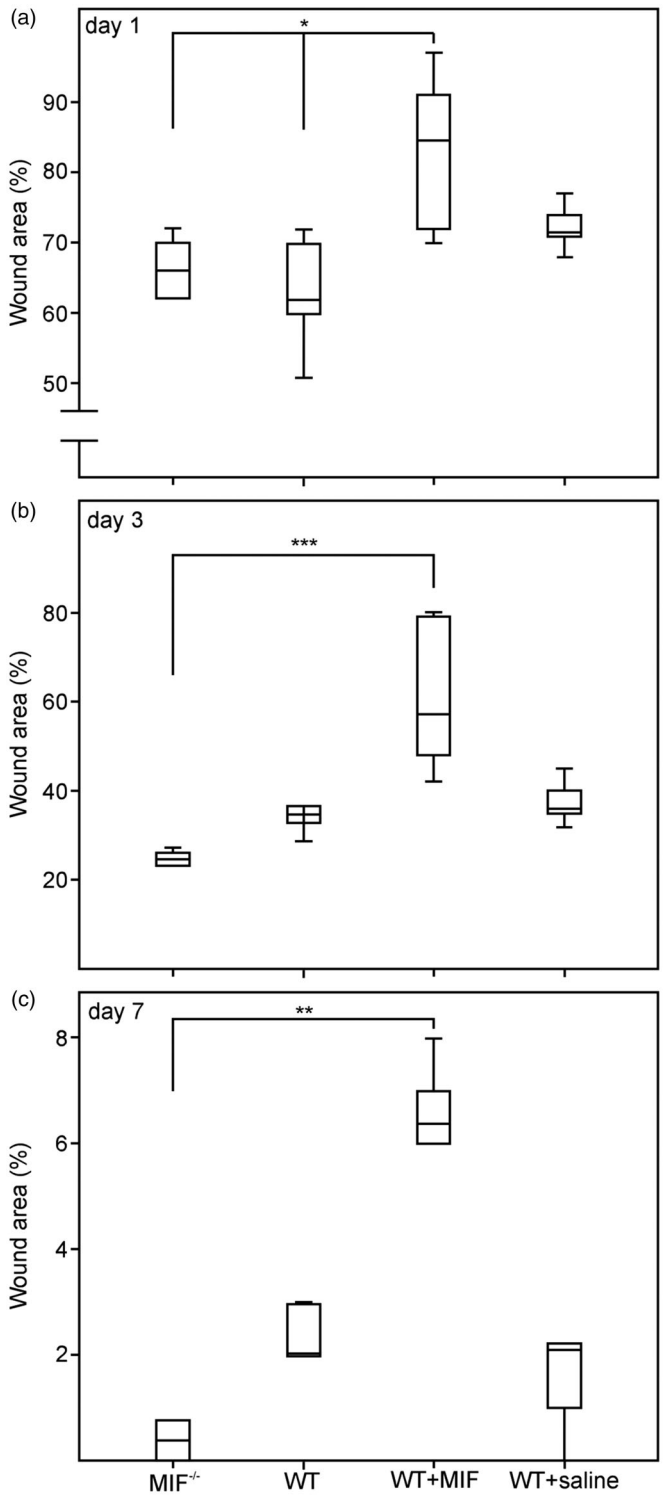

Figure 3. Wound area in the excisional wound model: Excisional wounds were placed on the back of the mice to investigate wound healing under regular perfusion. Dimensions of the excisional wounds of groups 1–4 were analyzed on days 1, 3 and 7 (each $n = 6$ per group) post-surgery (a–c). Wound sizes were calculated relative to initial values set as 100%. Statistical analysis was performed by the Kruskal–Wallis H-test followed by Mann–Whitney *U*-tests after Bonferroni correction; $^*p < 0.05$.

Results

Wound area

The wound area of the excisional wounds after the surgery was set as 100%. The wound repair progress was evaluated on days 1,

3, 7 and 14 after the surgery. For this purpose, healing wounds were measured for each animal and wound areas were calculated relative to initial values. In all animals, the wound area decreased over time (Figure 3). At day 1, wound size ranged between 62 – 84.5% (median) for all groups. Wounds of WT (62%) and *Mif*$^{-/-}$ (66%) mice were smaller when compared to saline (71.5%) and MIF (84.5%) injected mice (Figure 3(a)). MIF-injection led to significantly larger wound areas than in WT ($p < 0.05$) and *Mif*$^{-/-}$ mice ($p < 0.05$). On day 3, wound size of *Mif*$^{-/-}$ mice was reduced to 24.5% when compared to the initial size, while wound size of MIF injected mice was still at 57%. Measures of the remaining two groups ranged equally around 35–36% (Figure 3(b)). The *Mif*$^{-/-}$ mice displayed significantly smaller wound size than the MIF injected animals ($p < 0.001$). On day 7, wound areas were almost closed in all groups (0.4–6%), while the largest remaining wound area was found on MIF injected animals (6%). As found for the early days during the experiment, the wound areas of *Mif*$^{-/-}$ mice were significantly lower than found for MIF injected mice ($p < 0.01$). By day 14, the wounds of all mice were completely healed (data not shown). In general, for all post-surgery days the largest wounds were measured in MIF injected mice. Wounds of *Mif*$^{-/-}$ mice healed fastest, especially during the early time points of wound evaluation. WT mice always ranged in between the other two groups.

Expression of mac-3, TNFα, vWF

To further specify invaded cells as well as the inflammatory profile of excisional wounds and their potency of neo-vascularization, we performed immunofluorescence staining, calculated in percent of total area, against the macrophage surface marker Mac-3, the pro-inflammatory cytokine TNFα and the pro-angiogenic vWF.

On days 3, 7 and 14, tissue samples of the MIF-treated group showed significantly ($p < 0.05$) higher Mac-3 expression than the other three groups (Figure 4(a)). Samples of *Mif*$^{-/-}$ mice and saline controls were on similar levels on each day of testing, while values of WT animals were twice as high when compared to the former groups. However, on day 14 *Mif*$^{-/-}$ mice, WT and saline control mice showed similar Mac-3 expression which was significantly lower than in MIF injected mice ($p < 0.05$).

To verify the inflammatory state of the wounds, tissue samples were also stained for TNFα (Figure 4(b)). Wounds of MIF injected mice showed the highest TNFα staining over the course of the experiment. Statistical differences compared to all other three groups were found for day 3 and 7 ($p < 0.05$), while the effect was attenuated 14. On day 3, TNFα expression of saline control group was higher than in *Mif*$^{-/-}$ and WT mice, while on day 7 the samples of *Mif*$^{-/-}$ animals showed higher TNFα expression when compared to WT and saline control groups. However, these effects did not reach statistical significance

The least difference between the four groups was found in vWF expression. On day 3, the samples of MIF injected mice showed significantly higher vWF expression ($p < 0.05$) when compared to the MIF$^{-/-}$ and WT group (Figure 4(c)), while this effect was erased on day 7. On day 14, highest vWF expression was again seen in the MIF injected WT mice. This effect, however, was not significant.

Flap healing, blood flow, hemoglobin content and oxygen saturation under hypoxia

Healing of the flap was monitored as a measure of flap viability and perfusion. Oxygen deprivation due to the ischemic gradient

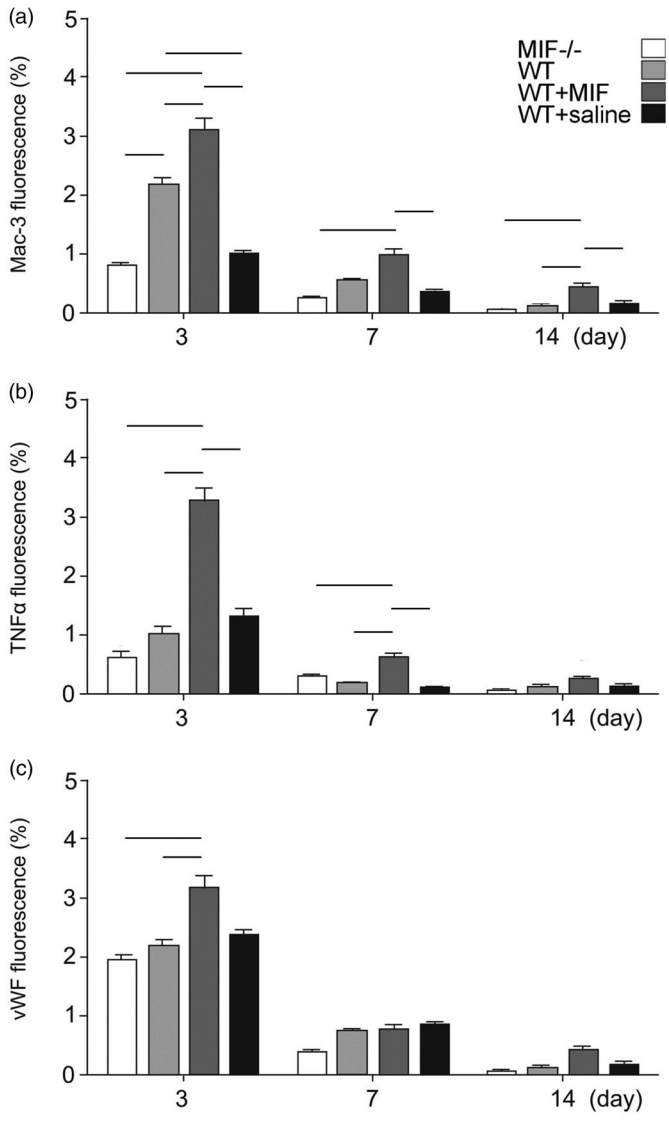

Figure 4. Mac-3, TNFα and vWF staining in the excisional wound model. Excisional wounds were placed on the back of the mice to investigate wound healing under regular perfusion. Expression of macrophage, pro-inflammatory and vascularization markers in the wounds were measured by immunofluorescent detection of Mac-3, TNFα and vWF in excised wound samples of two mice per group. Data were acquired from days 3, 7 and 14. Bars represent mean values (±SEM) of two measurements performed in samples of two mice each ($n = 4$). Statistical analysis was performed by the Kruskal–Wallis H-test followed by Mann–Whitney *U*-tests after Bonferroni correction; all bars indicate statistical significance with $^{*}p < 0.05$ between the marked columns.

in the flap led to hypoxia, which again caused tissue necrosis in distal parts of zone C. Tissue necrosis was identified as a dark discoloration of the skin in all animals. There was a regular increase in necrosis in both groups between days 3 and 7. The necrosis was consistent in both groups with no statistical difference (data not shown).

All flaps survived with no partial flap loss or other complications. Blood flow, hemoglobin content and oxygen saturation of the flap were evaluated by the non-invasive O_2C device. All values were acquired at four time points: before, directly after and on days 1 and 3 after the flap surgery.

The blood flow of the flaps indicated the transportation of blood to the injured tissue. Before the surgery, blood flow was similar level for both groups (69–72 arbitary units, AU). Immediately after surgery, blood flow dropped in all three flap

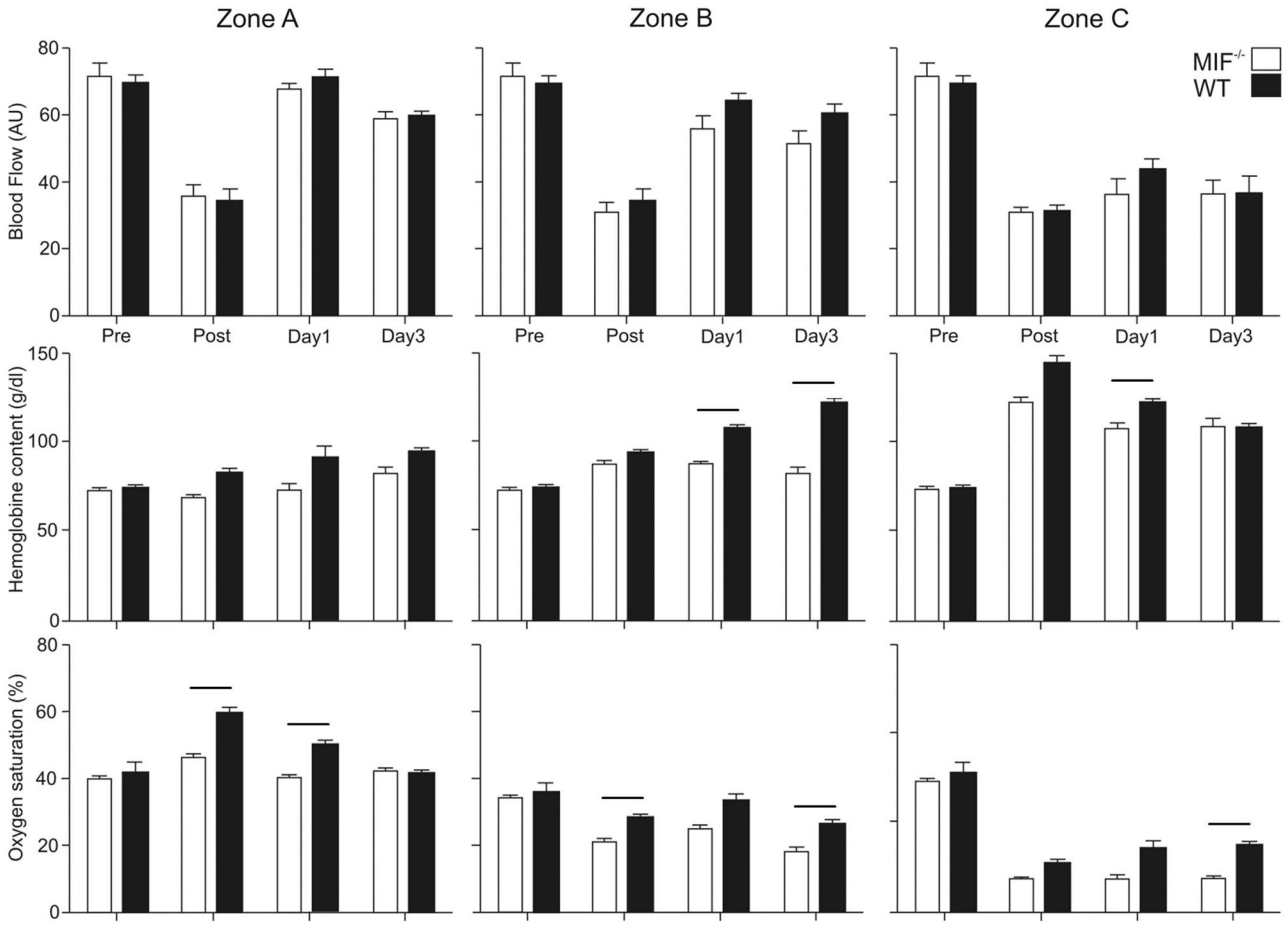

Figure 5. Blood flow, hemoglobin content and oxygen saturation as a measure of flap viability in the flap model. A random pattern flap was raised on the back of the mice to investigate wound healing under a perfusion gradient with maximum perfusion in zone A and least perfusion in zone C. Oxygen supply of the three zones of the flap indicated as a measure of blood flow, hemoglobin content and oxygen saturation in *Mif*$^{-/-}$ and WT mice. Data were acquired pre- and immediately post-surgery, and on days 1 and 3 after operation. Left column: zone A; central column: zone B; right column: zone C. First row: blood flow; second row: hemoglobin; third row: oxygen saturation. Bars represent mean values (±SEM) taken from one measure in each zone of six mice (each $n = 3$) at the indicated time points, no repeats; all bars indicate statistical significance with $^{*}p < 0.05$ between the marked columns.

zones in *Mif*$^{-/-}$ mice (A: 35 AU, B: 31 AU C: 31 AU) and WT animals (A: 34 AU, B: 35 AU C: 31 AU) but increased on the post-surgery days (Figure 5). While the blood flow recovered postoperatively in zones A and B, the values remained constantly low for zone C in both groups. There was a trend towards higher postoperative blood flow in WT mice for zone B, this effect however was statistically not significant.

The hemoglobin content correlates with the density and filling of the vascular system. Preoperatively, the hemoglobin level was similar in both groups (73 vs 74 g/dl, respectively). Immediately after the surgery as well as during subsequent wound healing, the hemoglobin level increased from zone A towards zone C (Figure 5). This effect was more obvious in WT mice when compared to *Mif*$^{-/-}$ mice. In flaps of WT animals, there was a steady increase in hemoglobin level over time for the zones A (post-surgery: 83 g/dl, day 1: 91 g/dl, day 3: 95 g/dl) and especially B (post-surgery: 94 g/dl, day 1: 108 g/dl, day 3: 121 g/dl), while levels in flaps of *Mif*$^{-/-}$ mice did not follow this trend and stayed on similar levels. For day 1 and 3, the difference for *Mif*$^{-/-}$ and WT mice was significant ($p < 0.05$). For zone C we found the strongest increase in hemoglobin content immediately after the surgery followed by a continuous decrease on days 1 and 3. Also, this effect was stronger in WT mice flaps (post-surgery: 144 g/dl, day 1: 122 g/dl, day 3: 108 g/dl) when compared to *Mif*$^{-/-}$ mice flaps (post-surgery: 121 g/dl, day 1: 108 g/dl, day 3: 109 g/dl). The difference between *Mif*$^{-/-}$ and WT mice was significant for day 1 ($p < 0.05$).

The oxygen saturation indicates the oxygen supply of wounded tissue. Preoperatively, oxygen saturation of the flaps was similar between both groups (Figure 5). Immediately after the surgery, there was an increase in oxygen saturation in zone A of flaps of WT animals (60%), while we found only a slight increase for flaps of *Mif*$^{-/-}$ mice (46%). On the other hand, oxygen levels dropped in zones B and C after the surgery, however, this effect was more pronounced in *Mif*$^{-/-}$ mice flaps (29% and 10%) when compared to WT mice flaps (39% and 19%). Overall, the oxygen levels tended to be higher in all zones of WT animals flaps when compared to *Mif*$^{-/-}$ mice flaps at any time. Statistical difference between *Mif*$^{-/-}$ and WT mice were seen for the post surgery time point in zone A and B, for day 1 in zone A and for day 3 in zone B and C ($p < 0.05$).

Discussion

Proper wound repair is of utmost interest to clinicians and while efforts to understand the exact pathophysiological processes were increased, the search for contributing factors still continues. Accruing evidence suggests that the ancient cytokine MIF plays a hitherto underappreciated role in cutaneous wound repair and healing of flaps although its precise effects remain unclear [12,18].

In excisional wounds, MIF slowed down wound healing and enhanced expression of the macrophage marker Mac-3, the pro-inflammatory cytokine TNFα and vWF was seen. Interestingly, there were less pronounced differences between *Mif*$^{-/-}$ and WT animals, whereas treatment with recombinant MIF produced the highest effect in all measured parameters. These observations suggest that a physiological concentration of MIF could have a less negative effect than pathologically increased MIF levels.

Our observation of MIF's detrimental effect on wound healing corroborates findings of others. *In vitro* scratch assays with fibroblasts treated by recombinant MIF for 24 h significantly reduced fibroblast migration [19]. Ashcroft et al. [16] reported that recombinant MIF significantly reduced wound healing in mice in an incisional wound healing model. Even though incisional and excisional wound models differ in their interpretability, these overlapping results are encouraging [20]. By contrast, other authors report a beneficial role of MIF in wound repair. Dewor et al. [21] observed a stimulation of fibroblast migration by MIF. This obvious contradictory results to Emmerson et al.'s work may be explained by the varying time of MIF exposure: Dewor et al. only observed enhanced fibroblast migration when recombinant MIF was added for two hours whereas longer periods had no comparable effects.

To characterize the effect of MIF on wound healing in more detail, we scrutinized three key aspects: macrophage count, expression of TNFα and vWF. Numerous studies have underlined MIF's paramount importance in mobilization of inflammatory cells in the past. Unlike its name, MIF facilitates the migration of monocytes/macrophages by its receptors CXCR2, CXCR4 and CD74 [3].

We observed significantly increased Mac-3 staining after MIF injection which suggests that MIF induced macrophage infiltration to the wound. In general, macrophages are divided into a pro-inflammatory M1 or an immuno-suppressive M2 phenotype [22]. Amongst many other cytokines, TNFα is a strong pro-inflammatory cytokine released predominantly by M1 macrophages. The increased MIF-dependent TNFα expression therefore may support the M1 macrophage polarization by MIF [23]. Our results suggest that MIF promotes inflammation in wound repair by mobilizing pro-inflammatory M1 macrophages which in turn secrete or up-regulate pro-inflammatory cytokines such as TNFα. MIF in fact is known as an up-stream regulator of TNFα [9]. However, as no co-stainings were performed and as no other M1 and M2 markers were measured, our hypothesis needs further validation.

In wounds, the formation of blood vessels is a prerequisite for successful healing. The down-regulation of vWF, an essential factor for cells of the microvascular endothelium, in *Mif*$^{-/-}$ mice in the excisional wound suggests a potential implication of MIF in neovascularization. An abundance of published work supports MIF's outstanding role in angiogenesis. For over two decades, scientists have elaborated on this aspect establishing firm evidence especially in tumor-associated neovascularization [24]. Despite the fact that mechanisms of tumor biology cannot be transferred directly to wound healing, some aspects might be relevant. In tumor progression macrophages derived from the bone marrow (BMDM) are recruited to the stroma and secrete MIF that dictates microvessel formation [25]. Moreover, MIF induces tumor neoangiogenesis by EPC recruitment [26]. MIF-related vWF expression may exert a cell-protective mechanism. This idea is supported by findings of Sauler et al. [27] describing a MIF-CD74-mediated protection against hyperoxic lung injury combined with a co-localization of CD74 and vWF. Hillgruber et al. [28] recently suggested vWF as a detrimental factor in cutaneous inflammation. Based on our experimental setup it is difficult to discern whether increased expression of vWF has a beneficial effect of MIF or a mere expression of increased tissue vascularization during inflammation. More detailed investigations with exact characterization of macrophage populations, investigation of other pro- and anti-inflammatory factors and scrutiny of blood vessel formation are planned.

In our flap model we aimed to investigate MIF's role in flap surgery. In contrast to the excisional wound, where the decrease of wound size is the primary goal, flap perfusion was set as the primary outcome in the flap model. While no difference in flap survival/amount of necrosis was seen, the flaps of *Mif* deficient mice presented reduced blood flow, hemoglobin content and oxygen tension.

One specific factor that may explain the potentially positive effect of MIF in the flap model is tissue hypoxia as flap perfusion also is connected to oxygen supply. Under hypoxic conditions, MIF was shown to induce migration of endothelial progenitor cells (EPCs) which in turn contribute to tissue vascularization [11]. The clinical relevance of MIF-induced EPC mobilization was demonstrated earlier, as patients after flap surgery showed a positive correlation between circulating MIF and EPC [12]. In the same vein, MIF activates the transcription factor HIF-1α through CD74 and Jab/CSN5 [29] and thereby activates proangiogenic factors such as CXCL8 and VEGF [30]. However, to underpin the importance of tissue hypoxia in the beneficial effect of MIF in wound healing, it requires additional experimental studies such as evaluation of HIF-1α action.

Aside from its potential use as a biomarker [8] there has been tremendous efforts to develop appropriate MIF antibodies or inhibitors, mostly to control immune diseases [31] or in cancer therapy [31]. MIF inhibition therefore also may be a relevant option for future therapeutic or tissue engineering approaches in wound healing.

Conclusion

MIF has a significant negative effect on excisional wounds *in vivo*. Also, significantly increased MIF-dependent inflammation as rendered by enhanced macrophage infiltration, TNFα expression and vascularization were seen. Under restricted perfusion, O_2C measurements indicated a beneficial effect of MIF in the context of tissue perfusion. The present work represents an initial effort in the evaluation of MIF in wound healing and flap perfusion and requires additional studies in the future.

Disclosure statement

The authors report no declarations of interest.

Funding

Bong-Sung Kim and Kevin Arnke were supported by the Deutsche Forschungsgemeinschaft (DFG) [KI1973/2-1]. Jürgen Bernhagen was supported by DFG grants [SFB 1123/A03, BE1977/7-1, BE1977/11-1].

References

[1] Sen CK. Wound healing essentials: let there be oxygen. Wound repair and regeneration: official publication of the Wound Healing Society [. And] the European Tissue Repair Society. 2009;17(1):1–18.

[2] Bloom BR, Bennett B. Mechanism of a reaction in vitro associated with delayed-type hypersensitivity. Science. 1966;153(3731):80–82.
[3] Bernhagen J, Krohn R, Lue H, et al. MIF is a noncognate ligand of CXC chemokine receptors in inflammatory and atherogenic cell recruitment. Nat Med. 2007;13(5):587–596.
[4] Tarnowski M, Grymula K, Liu R, et al. Macrophage migration inhibitory factor is secreted by rhabdomyosarcoma cells, modulates tumor metastasis by binding to CXCR4 and CXCR7 receptors and inhibits recruitment of cancer-associated fibroblasts. Mol Cancer Res. 2010;8(10): 1328–1343.
[5] Shi X, Leng L, Wang T, et al. CD44 is the signaling component of the macrophage migration inhibitory factor-CD74 receptor complex. Immunity. 2006;25(4):595–606.
[6] Leng L, Metz CN, Fang Y, et al. MIF signal transduction initiated by binding to CD74. The Journal of Experimental Medicine. 2003;197(11):1467–1476.
[7] Kindt N, Journe F, Laurent G, et al. Involvement of macrophage migration inhibitory factor in cancer and novel therapeutic targets. Oncology Letters. 2016;12(4): 2247–2253.
[8] Grieb G, Kim BS, Simons D, et al. MIF and CD74 - suitability as clinical biomarkers. MRMC. 2015;14(14):1125–1131.
[9] Rosado Jde D, Rodriguez-Sosa M. Macrophage migration inhibitory factor (MIF): a key player in protozoan infections. Int J Biol Sci. 2011;7(9):1239–1256.
[10] O'Reilly C, Doroudian M, Mawhinney L, et al. Targeting MIF in Cancer: Therapeutic Strategies, Current Developments, and Future Opportunities. Med Res Rev. 2016;36(3): 440–460.
[11] Simons D, Grieb G, Hristov M, et al. Hypoxia-induced endothelial secretion of macrophage migration inhibitory factor and role in endothelial progenitor cell recruitment. J Cell Mol Med. 2011;15(3):668–678.
[12] Grieb G, Piatkowski A, Simons D, et al. Macrophage migration inhibitory factor is a potential inducer of endothelial progenitor cell mobilization after flap operation. Surgery. 2012;151(2):268–277 e1.
[13] Kim BS, Rongisch R, Hager S, et al. Macrophage Migration Inhibitory Factor in Acute Adipose Tissue Inflammation. PLoS One. 2015;10(9):e0137366.
[14] Shimizu T, Ohkawara A, Nishihira J, et al. Identification of macrophage migration inhibitory factor (MIF) in human skin and its immmunohistochemical localization. FEBS Letters. 1996;381(3):199–202.
[15] Gilliver SC, Emmerson E, Bernhagen J, et al. MIF: a key player in cutaneous biology and wound healing. Experimental Dermatology. 2011;20(1):1–6.
[16] Ashcroft GS, Mills SJ, Lei K, et al. Estrogen modulates cutaneous wound healing by downregulating macrophage migration inhibitory factor. J Clin Invest. 2003;111(9): 1309–1318.
[17] Foltynski P, Ladyzynski P, Ciechanowska A, et al. Wound Area Measurement with Digital Planimetry: Improved Accuracy and Precision with Calibration Based on 2 Rulers. PloS One. 2015;10(8):e0134622.
[18] Gilliver SC, Emmerson E, Bernhagen J, et al. MIF: a key player in cutaneous biology and wound healing. Exp Dermatol. 2011;20(1):1–6.
[19] Emmerson E, Campbell L, Ashcroft GS, et al. Unique and synergistic roles for 17beta-estradiol and macrophage migration inhibitory factor during cutaneous wound closure are cell type specific. Endocrinology. 2009;150(6): 2749–2757.
[20] Ansell DM, Campbell L, Thomason HA, et al. A statistical analysis of murine incisional and excisional acute wound models. Wound repair and regeneration: official publication of the Wound Healing Society. Wound Repair Regen. 2014; 22(2):281–287.
[21] Dewor M, Steffens G, Krohn R, et al. Macrophage migration inhibitory factor (MIF) promotes fibroblast migration in scratch-wounded monolayers in vitro. FEBS Letters. 2007; 581(24):4734–4742.
[22] Cassetta L, Cassol E, Poli G. Macrophage polarization in health and disease. TheScientificWorldJournal. 2011;11: 2391–2402.
[23] Lumeng CN, Bodzin JL, Saltiel AR. Obesity induces a phenotypic switch in adipose tissue macrophage polarization. J Clin Invest. 2007;117(1):175–184.
[24] Chesney JA, Mitchell RA. 25 Years On: A Retrospective on Migration Inhibitory Factor in Tumor Angiogenesis. Mol Med. 2015;21(S1):S19–S24.
[25] Wang X, Chen T, Leng L, et al. MIF produced by bone marrow-derived macrophages contributes to teratoma progression after embryonic stem cell transplantation. Cancer Research. 2012;72(11):2867–2878.
[26] White ES, Strom SR, Wys NL, et al. Non-small cell lung cancer cells induce monocytes to increase expression of angiogenic activity. J Immunol. 2001;166(12):7549–7555.
[27] Sauler M, Zhang Y, Min JN, et al. Endothelial CD74 mediates macrophage migration inhibitory factor protection in hyperoxic lung injury. Faseb J. 2015;29(5):1940–1949.
[28] Hillgruber C, Steingraber AK, Poppelmann B, et al. Blocking von Willebrand factor for treatment of cutaneous inflammation. J Invest Dermatol. 2014;134(1):77–86.
[30] Oda S, Oda T, Nishi K, et al. Macrophage migration inhibitory factor activates hypoxia-inducible factor in a p53-dependent manner. PloS One. 2008;3(5):e2215.
[31] Xu X, Wang B, Ye C, et al. Overexpression of macrophage migration inhibitory factor induces angiogenesis in human breast cancer. Cancer Letters. 2008;261(2):147–157.
[32] Kok T, Wasiel AA, Cool RH, et al. Small-molecule inhibitors of macrophage migration inhibitory factor (MIF) as an emerging class of therapeutics for immune disorders. Drug Discovery Today. 2018;23(11):1910–1918.